

How surface latent heat flux is related to lower-tropospheric stability in southern subtropical marine stratus and stratocumulus regions

Research Article

Yanping He*

School of Earth and Ocean Science, University of Victoria, Victoria, BC, V8W3P6, Canada

Received 28 June 2009; accepted 20 July 2009

Abstract: The relationship between surface latent heat flux and the lower-tropospheric stability (LTS) is examined using ERA-40 reanalysis, NCEP reanalysis and COADS (Comprehensive Ocean-Atmosphere Data Set) ship data in two southern subtropical marine stratus and stratocumulus regions. The change of surface latent heat flux with LTS is determined by a comparison of the correlation of LTS with surface wind speed and with near surface humidity difference. At intermediate LTS (10 K-15 K), both surface evaporation and downward surface radiation flux amplify small LTS perturbations due to the surface wind-LTS relationship and cloud-radiation feedback. At high LTS, surface latent heat flux exceeds its peak value and becomes a regulating mechanism to keep LTS at its commonly observed equilibrium value. Surface radiation flux is seen to decrease at a smaller rate with LTS than surface latent heat flux. By applying the regulating effect of LTS on near surface humidity differences, monthly surface latent heat flux can be better represented.

Keywords: latent heat flux • lower tropospheric stability • ERA-40 • NCEP • COADS

© Versita Warsaw

1. Introduction

The importance of subtropical surface latent heat flux for marine boundary layer clouds, tropical circulation and air-sea interaction is widely appreciated. Simulation of the ocean surface flux and air-sea coupling requires an understanding of what controls and regulates latent heat fluxes. The subtropical lower troposphere is characterized by a strong temperature inversion, persistent marine stratus and stratocumulus (MSC), and large surface latent heat fluxes. This rather stable equilibrium is a result of a

subtle balance between the circulation, cloud field, surface winds, and ocean surface temperature within the atmospheric boundary layer. The lower-tropospheric stability $\Delta\theta$ (LTS), is important for subtropical ocean-atmosphere-cloud interaction and is defined here as the difference between the 700 hpa potential temperature θ_{700} and ocean surface temperature *SST*.

Lilly [1] proposed that cloud-top radiative cooling associated with a strong temperature inversion is important for maintaining the cloud topped boundary layer. Betts and Ridgway [2, 3] investigated through an equilibrium solution, how large-scale subsidence and radiative forcing control the surface latent heat flux. A positive relationship between marine low cloud amounts and LTS in daily to seasonal timescales, was found in previous studies [4-7].

*E-mail: ghe@uvic.ca

Controls on surface latent heat flux have largely been examined in terms of SSTs, tropical convection and surface winds. The intent of this study is to show how surface latent heat flux is linked to LTS. This nonlinear relationship explains why lower tropospheric stability is quite stable in the subtropics.

Strong cloud-top radiative cooling enhances the lower tropospheric pressure gradient [8, 9], leading to the observed local positive feedback between surface wind and LTS in subtropical MSC regions. This feedback is different from the mechanism proposed to explain unstable low-frequency variability within the tropical atmosphere [10], in which the zonal wind anomaly leads to a surface evaporation anomaly so that the low frequency wave growth is supported by drawing moist static energy from the fixed SST. It is also different from the feedback proposed by Clarke and Lebedev [11] in which near surface ocean coastal wind is accelerated due to horizontal pressure differences and boundary layer height variations.

In the subtropics, the colder the SST, the higher the LTS, the larger the marine low cloud cover and the weaker the solar flux that reaches the ocean surface, all providing a positive feedback between cloud cover and SST. If humidity differences were to dominate surface latent heat flux variations, as suggested for equatorial cold regions [12], then the combination of marine low cloud cover-SST feedback and the thermodynamic effects of SST on saturation specific humidity would imply a local negative relationship between surface evaporation and LTS. However, a positive feedback among surface wind, surface latent heat flux and MSC cloud-top radiative cooling was proposed to explain the seasonal transition near the Peruvian region in a diagnostic model study [13].

The results of this paper unify the previous observations by suggesting that a positive relationship should be found for low LTS and a negative relationship for high LTS, and that these two opposing feedbacks, combined with cloud-radiation-LTS feedback, will determine a peak in the most frequent value of LTS. A modified bulk formula based on surface wind and LTS is introduced in Section 3, which is shown to improve monthly averaged surface latent heat flux in subtropical MSC regions. In Section 4, we interpret the preferred value of LTS as a simple dynamic system with an unstable fixed point and a stable fixed point.

2. Data description

Surface latent heat flux F_{LH} , specific humidity at 2 m q_a and surface wind speed at 10 m U_a , were obtained from daily ECMWF 40-Year Re-analysis (ERA-40), daily National Centers of Environmental Prediction (NCEP) and

Table 1. The geographical extent of two subtropical MSC regions considered in the study.

Regions	Locations
Peruvian	(5S–20S, 80W–95W)
Namibian	(5S–20S, 5W–10E)

National Centers for Atmospheric Research (NCAR), re-analysed as physically consistent datasets with continual coverage in time and space. The daily LTS in the ERA-40 reanalysis was calculated from the International Satellite Cloud Climatology Projects Radiation Flux Dataset (ISCCP-FD), sea surface temperature [14] and ERA-40 air temperature at 700 hpa. LTS in the NCEP NCAR reanalysis is calculated from the NCEP NCAR ocean surface SST and air temperature at 700 hpa. The monthly surface radiation flux dataset is obtained from the ISCCP FD dataset with $2.5^\circ \times 2.5^\circ$ horizontal resolution. Ship data from COADS has passed through various data quality checks and though useful for climatology studies, its sampling is irregular in both time and space. Individual data are contained within a spatial grid of $2.5^\circ \times 2.5^\circ$ resolution before being averaged into monthly values there are more than 10 observations within each grid cell for that month. Table 1 shows the geographic locations of the southern subtropical MSC regions under consideration. The study period ranges from January 1985 to December 1997, when both the COADS dataset and ISCCP-FD dataset are available. There are 336,960 daily grid-point data and 11,232 monthly grid-point data in each re-analysis. Over half a million individual COADS ship data were processed into 3,578 monthly grid-point observations. The COADS dataset is sufficient for statistically robust results of the relationship between LTS and single surface variable in Section 3 but is not used to quantify the surface latent heat-LTS relationship because of the larger data volume and continuity, in both time and space, necessary for higher order variables.

3. Results

3.1. Surface latent heat flux and the lower-tropospheric stability

Figure 1 shows the monthly surface latent heat flux and downward surface radiation flux (SRF), as a function of monthly LTS estimated using temperature bin widths of 0.25 K over two MSC regions (from 1985 to 1997) using two re-analysed ISCCP FD datasets. The number of

months found in each of these temperature bins is also plotted against the two re-analysed datasets in Figure 1. At intermediate LTS (10K-15K), ERA-40 monthly surface latent heat flux slightly increased before it reached a peak at 140 Wm^{-2} while the NCEP NCAR monthly surface latent heat flux increased with LTS at a rate of $4 \text{ Wm}^{-2}\text{K}^{-1}$. At high LTS, surface latent heat flux from these data sets decreases at a rate of $-3.5 \text{ Wm}^{-2}\text{K}^{-1}$ and $-6 \text{ Wm}^{-2}\text{K}^{-1}$, respectively. ISCCP FD SRF decreases at a rate of $-2 \text{ Wm}^{-2}\text{K}^{-1}$ when LTS is less than 18 K but remain rel-

atively unchanged when LTS is between 18 K and 22 K. More than 50% of the occurrences of LTS fall around its peak value within 16 K and 20 K in ERA-40 and within 16 K and 18 K in NCEP NCAR reanalyses. Values very far beyond these ranges are much less frequent for reasons discussed in Section 4. Figure 1 shows that LTS has a broader distribution in the ERA-40 reanalysis than in the NCEP reanalysis. The ERA-40 LTS is derived from the satellite based ISCCP D-series dataset, which has more variability in MSC regions than that used by NCEP.

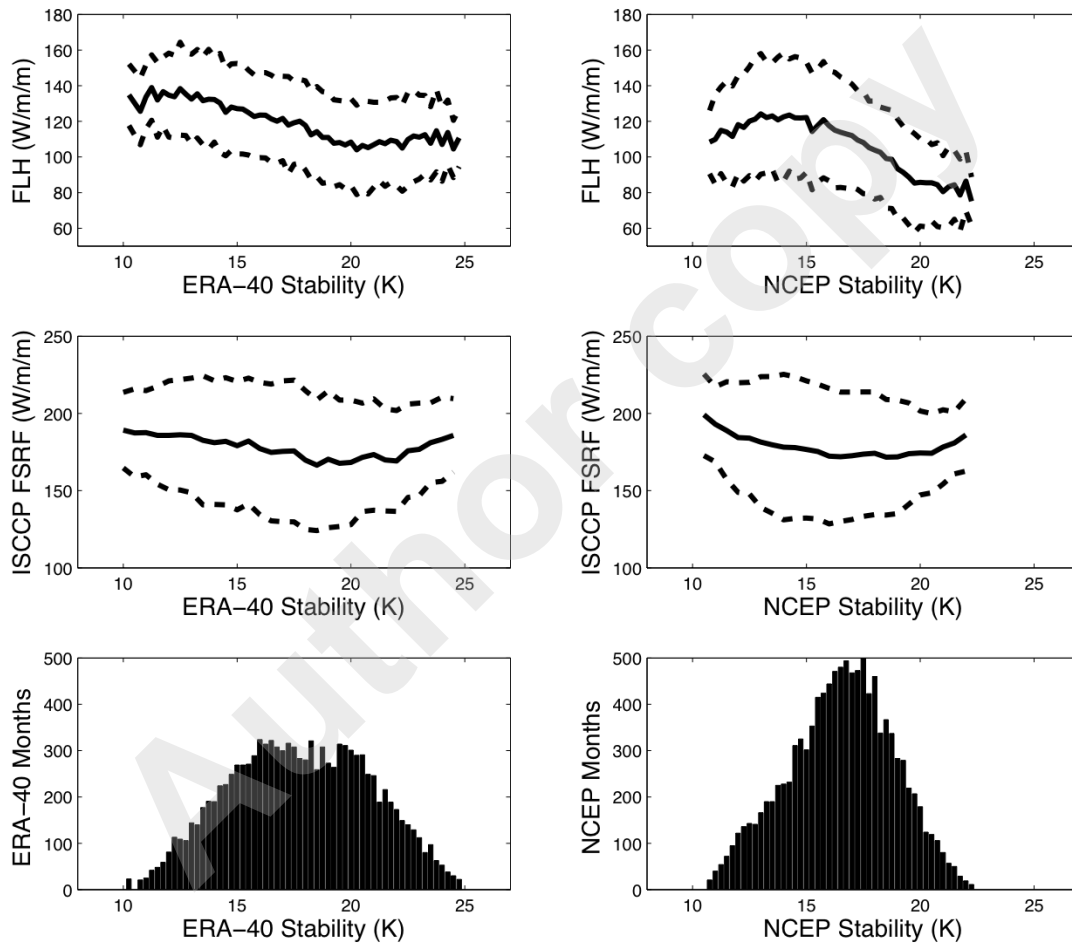


Figure 1. The monthly surface evaporation (Wm^{-2}) (upper panel) and the monthly ISCCP FD net downward surface radiation flux (Wm^{-2}) (middle panel) are displayed as a function of monthly atmosphere stability (0.25 K bin width) from ERA-40 reanalysis data (upper left) and NCEP-NCAR reanalysis data (upper right) in two MSC regions over the period from 1985 to 1997. The solid line represents mean values; and the dashed lines represent standard deviations. The lower panel is the number of observed months that lower tropospheric stability falls into a bin box with 0.25 K widths.

Figure 1 illustrates the non-linear dependence of fluxes on stability that this study addresses. Surface evaporation is

commonly based on the following bulk formula:

$$F_{LH} = L_v \rho C_e U_a (q_s - q_a), \quad (1)$$

where L_v is latent heat of condensation, C_e is the surface exchange coefficient for moisture, U_a is the surface wind speed, q_s is the saturated specific humidity at ocean surface and q_a is the air specific humidity at 2 m above the

surface. Monthly surface wind speeds and near surface humidity differences at 2 m are plotted as functions of monthly LTS in Figure 2, as estimated with a 0.25 K bin width based on daily ERA-40 (left panel) and NCEP-NCAR (right panel) re-analysed data in subtropical MSC regions during the period from 1985 to 1997.

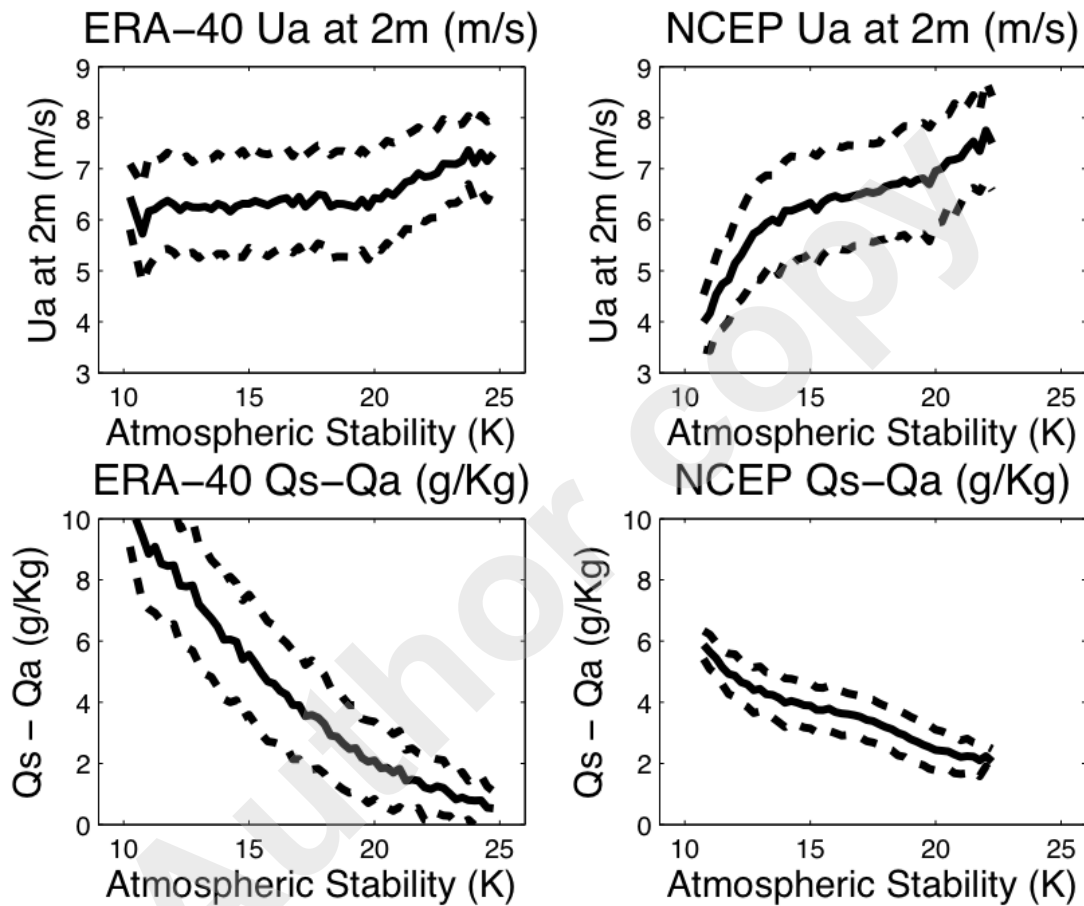


Figure 2. Monthly wind speed at 2 m U_a (ms^{-1}) (upper panel) and Δq (g(Kg)^{-1}) (lower panel) as a function of monthly $\Delta\theta$ (0.25 K bin width) from the ERA-40 (left panel) and the NCEP (right panel) in two subtropical MSC regions during the period from 1985 to 1997. The solid line represents mean values; and the dashed lines represent standard deviations.

A nearly linear positive relationship between re-analysed surface wind speed and the stability LTS is suggested by the re-analysed data in all subtropical MSC regions. The monthly surface wind speed increases at approximately 0.1 to 0.2 ms^{-1} for every 1 K increase of LTS. The NCEP reanalysis monthly surface wind increases rapidly at both low and high LTS while the ERA-40 surface wind in-

creases mainly at high LTS. Figure 2 shows the monthly humidity difference Δq , had a strong negative correlation with monthly LTS from 1985 to 1997. The ERA-40 Δq decreases with LTS at a rate of around $0.6 \text{ g(Kg)}^{-1}\text{K}^{-1}$ and the corresponding NCEP values are approximately $0.2 \text{ g(Kg)}^{-1}\text{K}^{-1}$ in two MSC regions, a consequence of the colder SST and moister near surface air in the low LTS

regime of the NCEP re-analyses; but warmer SST and drier near surface air in the high stability regime. Both datasets display a negative linear relationship between Δq and LTS. In subtropical MSC regions, the humidity difference Δq , is not only controlled by the SST but also by a relationship between the near surface relative humidity and LTS.

It is worth noting that in the two re-analyses, surface wind speed and near surface specific humidity is vertical extrapolated from their model's bottom level value. It depends on both observations and model physical schemes.

Due to different boundary layer schemes and vertical extrapolation formulas implemented in ERA40 and NCEP-NCAR models, the relationships of U_o and Δq with LTS show differences between two re-analyses, as illustrated in Figure 2. However, basic linear trends of monthly U_o and Δq with LTS are shown in both re-analysed datasets, which are supported by COADS ship observations displayed in Figure 3. This suggests that the mechanisms of LTS affecting surface latent heat flux are reasonably described by the two re-analysed model simulations.

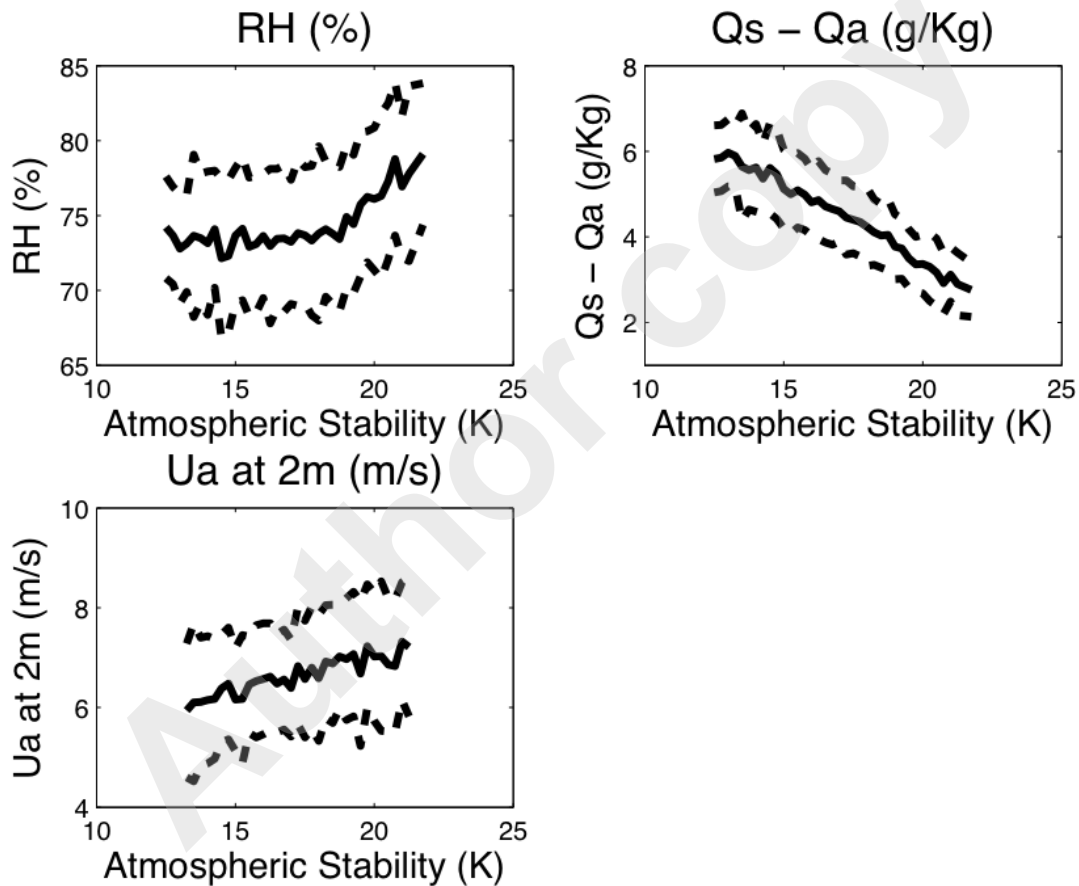


Figure 3. Monthly near surface relative humidity at 2 m RH (%) (upper left), specific humidity difference $(q_s - q_a)$ $(\text{g/Kg})^{-1}$ (upper right), and wind speed at 2 m (lower left) as functions of monthly LTS from the COADS ship data and the ERA-40 reanalysis during the period from 1985 to 1997 in two subtropical MSC regions.

Figure 3 shows COADS monthly values of near surface humidity at 2 m RH (%), Δq $(\text{g/Kg})^{-1}$ and U_o (m/s), as functions of ERA-40 monthly LTS from 1985 to 1997. COADS RH increases particularly at moderate and high LTS; Δq

decreases linearly at a rate of around $0.5 (\text{g/Kg})^{-1} \text{K}^{-1}$ and U_o increases linearly at a rate of around $0.15 \text{ms}^{-1} \text{K}^{-1}$. Stronger stability prevents the warm and dry free air from mixing into the boundary layer and enhances the mois-

ture transport from the surface, raising the near surface relative humidity.

3.2. Representing latent heat flux as functions of surface wind speed and lower-tropospheric stability

The bulk formula as shown for the latent heat flux, Equation (1), is a widely used parameterization for climate models. It requires an input of near surface specific humidity q_a , which is controlled by both large-scale deterministic and small-scale random processes. Currently, the marine boundary layer cloud schemes and turbulence parameterizations of climate models have major weaknesses; their realistic simulation of near surface air specific humidity is problematical but lower-tropospheric stability is more accurately simulated in most current GCMs. The linear relationship between near surface humidity difference Δq

and LTS as shown in both Figure 2 and Figure 3, can be introduced into the bulk formula of Equation (1) as follows:

$$F_{LH} = L_v \rho C_e U_a \Delta q_0 (1 - \Delta\theta/\Delta\theta_{\max}), \quad (2)$$

where $\Delta\theta_{\max} = -\Delta q_0/(\Delta q/\Delta\theta)$, denoting the value at which the surface latent heat flux becomes negative. The C_e , Δq_0 , and $\Delta\theta_{\max}$ are empirical values obtained by a least squares fit of daily ERA-40 and ISCCP D-series SST data from 1985 to 1989. Monthly surface latent heat flux is calculated either by the traditional bulk formula of Equation (1) or by the new formula in Equation (2), using daily fields from 1990 to 1997. The ERA-40 surface latent heat flux is a product of ocean surface observations combined with operational model output. The short-time observations and model output within a given time period are averaged to monthly values.

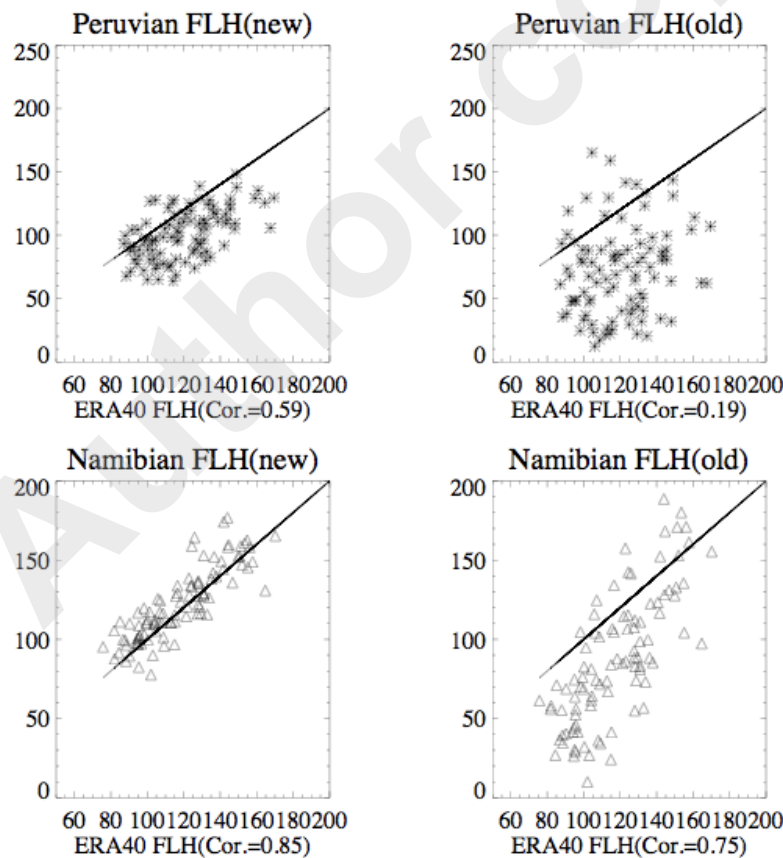


Figure 4. Area averaged monthly-simulated surface latent heat flux plotted against the ERA-40 monthly surface latent heat flux in subtropical MSC regions during the period from 1990 to 1997. In the left panel, the surface flux is a function of surface wind speed and stability as in Equation (2); and in the right panel, the flux is a function of surface wind speed, and specific humidity difference as in Equation (1) assuming constant surface drag coefficient C_e . Symbols: Peruvian (asterisk), Namibian (triangle).

Figure 4 shows area averaged monthly-simulated surface latent heat flux plotted against ERA-40 monthly surface latent heat flux in subtropical MSC regions from 1990 to 1997. The left panel shows the surface flux that is determined from the new scheme in Equation (2) using surface wind speed and LTS. The right panel, shows surface flux determined by surface wind speed and specific humidity difference as in Equation (1), assuming a constant surface drag coefficient C_e . The new formula simulates a better surface latent heat flux than that of the traditional bulk formula in most subtropical MSC regions. The explained covariance of monthly surface evaporation is improved from 4% to 35% near the Peruvian region and from 56% to 72% near the Namibian region. It is worth noting that this empirical formula is designed to better represent monthly surface latent heat flux; it is not designed to replace traditional bulk formula in calculating surface flux at shorter time scales (for example every 20-minutes) in most GCMs.

4. Discussion

Surface fluxes in numerical models and from satellite retrievals on short timescales commonly obtain surface latent heat flux from surface wind speed U_o and air-sea humidity difference Δq using Equation (1). This paper shows that this flux can be related to LTS by the sensitivity of U_o and Δq to LTS, i.e.:

$$\frac{\partial F_{LH}}{\partial \Delta \theta} = L_v \rho C_e \left(\Delta q \frac{\partial U_o}{\partial \Delta \theta} + U_o \frac{\partial \Delta q}{\partial \Delta \theta} \right). \quad (3)$$

When $\Delta \theta$ is small, U_o is also relatively small and Δq is large, and the change of surface latent heat flux with time is primarily determined by a positive feedback between local surface wind and the stability as shown in the first term on the right side of Equation (3). Cross correlation analysis on daily timescales suggests that both ERA-40 and NCEP NCAR surface wind speed variations lead LTS variation by approximately 2 days. An increase of the former can quickly enhance the latter through a positive relationship between them. However, in moderate and high stability regimes, U_o is large and Δq is relatively small. Under these conditions the relationship between latent heat flux and LTS is mainly determined by the negative relationship between the near surface humidity difference and LTS.

How LTS is related to surface latent heat flux, as shown in Figure 1, can be described conceptually by a first order dynamic system. The time tendency of LTS is:

$$\frac{d\Delta \theta}{dt} = Y(\Delta \theta) = \alpha F_{LH}(\Delta \theta) - R(\Delta \theta) + S_0, \quad (4)$$

where α is a positive parameter that also includes surface sensible heat flux effect, S_0 is a constant remaining source term and R is the net radiative effect, which represents the dependence of surface downward radiation flux (SRF) on LTS due to cloud-radiation feedback. Persistent marine low cloud exists in moderate and high LTS regions. It reduces surface shortwave flux due to strong cloud albedo effect, but it increases downward longwave radiation flux toward ocean surface. The net SRF is reduced because the SW effect dominates the LW effect. Cloud-radiation-LTS relationship implies a positive SRF-LTS feedback. Such a dynamical system with dependence of F_{LH} and SRF on the stability LTS, as shown in Figure 1, has two fixed points: one unstable and one stable. The curve of $Y(\Delta \theta)$ is characterized by an increase of $Y(\Delta \theta)$ with LTS, when LTS is small, and a decrease of $Y(\Delta \theta)$ with LTS when LTS is large. The unstable fixed point occurs in relatively small LTS regimes when both surface evaporation and SRF have positive feedbacks with LTS. A small increase of surface evaporation or marine low cloud amount amplifies the LTS perturbation, pushing it away from its original value. This instability is consistent with the sudden increases of surface evaporation, LTS and MSC cloud amounts during the seasonal transition near the Peruvian region [13]. Once, surface latent heat flux reaches peak value, a further increase of LTS leads to reduced latent heat flux, which results in an SST increase. It can be seen from Figure 1 that both ERA-40 and NCEP NCAR monthly surface latent heat flux decrease at a larger rate than that of SRF in the LTS range between 15 K and 22 K. This implies that the regulating effect of surface latent heat flux plays the dominant role, pushing the system back into its stable fixed point at high LTS regime. This mechanism explains why, in Figure 1, the observed latent heat flux reaches its maximum at a smaller LTS value (around 14 K in NCEP), while LTS has its most frequently occurring value between approximately 16 K and 18 K.

5. Conclusions

This paper examines the relationship between surface latent heat flux and lower tropospheric stability using ERA-40 reanalysis, the NCEP NCAR reanalysis and COADS ship data over the period from 1985 to 1997, in two MSC regions. Changes in surface wind and near surface humidity differences determine surface latent heat flux variations. The positive feedback of both surface evaporation and SRF with LTS implies that the latter has one unstable point at intermediate LTS, between 10 K and 15 K. At high LTS, the decrease of surface latent heat flux is observed to be larger than the decrease of SRF, suggesting that

a stable point may exist at high LTS. The area-averaged monthly surface latent heat flux is best simulated by daily averaged surface wind and the dependence of near surface humidity on LTS near the Peruvian and Namibian regions. The contribution of ocean dynamical transport is included in the remaining source term S_0 in the Eq. (4), which plays a compatible role in the variations of lower tropospheric stability only in low MSC seasons. How does ocean dynamical transport influence LTS will be investigated in a future study.

Acknowledgements

The author greatly thanks Dr. Robert E. Dickinson in University of Texas, Austin, and Dr. Adam Hugh Monahan in University of Victoria for insights, suggestions and improvements. This work was supported by NSF No. ATM 0343485. The author is grateful to Dr. Y. C. Zhang for providing huge ISCCP FD datasets and promptly responding to our queries. Special thanks go to Dr. Robert Wood, the University of Washington, for greatly improving the quality of this paper.

References

- [1] Lilly D.K., Models of Cloud-Topped Mixed Layers under a Strong Inversion, *Q. J. Roy. Meteor. Soc.*, 1968, 94, 292–309
- [2] Betts A.K., Ridgway W., Coupling of the Radiative, Convective, and Surface Flux over the Equatorial Pacific, *J. Atmos. Sci.*, 1988, 45, 522–536
- [3] Betts A.K., Ridgway W., Climate Equilibrium of the Atmospheric Convective Boundary Layer over a Tropical Ocean, *J. Atmos. Sci.*, 1989, 46, 2621–2641
- [4] Slingo J. M., A cloud parameterization scheme derived from GATE data for use with a numerical model, *Q. J. Roy. Meteor. Soc.*, 1980, 106, 747–770
- [5] Slingo J.M., The development and verification of a cloud prediction scheme for the ECMWF model, *Q. J. Roy. Meteor. Soc.*, 1987, 113, 899–927
- [6] Klein S. A., Hartmann D. L., The Seasonal Cycle of Low Stratiform Clouds, *J. Climate*, 1993, 6, 1587–1606
- [7] Wood R., Hartmann D.L., Spatial Variability of Liquid Water Path in Marine Boundary Layer Clouds. Part I: the Importance of Mesoscale Cellular Convection, *J. Climate*, 2006, 19, 1748–1764
- [8] Tian B., Ramanathan V., A Simple Moist Tropical Atmosphere Model: The Role of Cloud Radiative Forcing, *J. Climate*, 2003, 16, 2086–2092
- [9] He Y., Representations of Boundary Layer Cloudiness and Surface Wind Probability Distributions in Sub-tropical Marine Stratus and Stratocumulus Regions, PhD thesis, Georgia Institute of Technology, USA, 2007
- [10] Neelin J.D., Held I.M., Cook K.H., Evaporation-Wind Feedback and Low-Frequency Variability in the Tropical Atmosphere, *J. Atmos. Sci.*, 1987, 44, 2341–2348
- [11] Clarke A.J., Lebedev A., Interannual and Decadal Changes in Equatorial Wind Stress in the Atlantic, Indian, and Pacific oceans and the Eastern Ocean Coastal Response, *J. Climate*, 1997, 10, 1722–1729
- [12] Zhang J.G., McPhaden M.J., The Relationship between Sea Surface Temperature and Latent Heat Flux in the Equatorial Pacific, *J. Climate*, 1995, 8, 589–605
- [13] Nigam S., The Annual Warm to Cold Phase Transition in the Eastern Equatorial Pacific: Diagnosis of the Role of Stratus Cloud-Top Cooling, *J. Climate*, 1997, 10, 2447–2467
- [14] Zhang Y.C., Rossow W., Lacis A.A., Oinas V., Mishchenko M.I., Calculation of Radiative Fluxes from the Surface to Top of Atmosphere based on ISCCP and Other Global Datasets: Refinements of the Radiative Transfer Model and the Input Data, *J. Geophys. Res.*, 2004, 109, D19105